

# Intermolecular Interactions on Amine-Cured Epoxy Matrices with Different Crosslink Densities. Influence on the Hole and Specific Volumes and the Mechanical Behavior

M. BLANCO,<sup>1</sup> J. A. RAMOS,<sup>1</sup> S. GOYANES,<sup>2,3</sup> G. RUBIOLLO,<sup>2,3,4</sup> W. SALGUEIRO,<sup>5</sup> A. SOMOZA,<sup>5,6</sup> I. MONDRAGON<sup>1</sup>

<sup>1</sup>Materials + Technologies Group, Dpto Ingeniería Química y M Ambiente, Escuela Politécnica, Universidad País Vasco/Euskal Herriko Unibertsitatea, Pza, Europa 1, 20018 Donostia-San Sebastián, Spain

<sup>2</sup>Laboratorio de Polímeros y Materiales Compuestos, FCEyN, Universidad de Buenos Aires, Pabellón 1 Ciudad Universitaria, Buenos Aires 1424, Argentina

<sup>3</sup>CONICET, Consejo Nacional de Investigaciones Científicas y Tecnológicas, Argentina

<sup>4</sup>Unidad de Actividad Materiales, Comisión Nacional de Energía Atómica, Avenida General Paz 1499, B1650KNA San Martín, Argentina

<sup>5</sup>Instituto de Física de Materiales Tandil, Universidad Nacional del Centro de la Provincia de Buenos Aires, Pinto 399, B7000GHG, Argentina

<sup>6</sup>Comisión de Investigaciones Científicas de la Provincia de Buenos Aires, Pinto 399, B7000GHG, Argentina

Received 8 May 2008; revised 2 April 2009; accepted 3 April 2009

DOI: 10.1002/polb.21729

Published online in Wiley InterScience (www.interscience.wiley.com).

**ABSTRACT:** The architecture of an epoxy matrix was modified by curing the resin with mono-/diamine mixtures having identical chemical structures. Both hole volume and specific volume variations were studied by positron annihilation lifetime spectroscopy and pressure-volume-temperature/density measurements, respectively. The average hole volume of the networks at room temperature slightly increased when the monoaminic chain extender content increased. The increment in the intermolecular interactions between functional groups of the networks chains, due to the less hindered nitrogen introduced by the monoamine, appears to be the responsible for the observed behavior. Besides, only small variations on the specific volume were observed on increasing the monoamine content, which points out that for a cured epoxy system, the chemical structure of the curing agent is mainly responsible for chain packing in the networks. On the other hand, intermolecular interactions between chains were considered as the key factor for fixing stiffness and strength. Thus, it was observed that the increase of the intermolecular interactions with the monoamine content produced a decrease in the sub- $T_g$  small-range cooperative motions, which increased the low-deformation mechanical properties at temperatures between  $\beta$  and  $\alpha$  relaxations. This conclusion could be applied to previous investigations with epoxy matrices not fully crosslinked (nonstoichiometric or noncompletely

---

Correspondence to: I. Mondragon (E-mail: inaki.mondragon@ehu.es)

Journal of Polymer Science: Part B: Polymer Physics, Vol. 47, 1240–1252 (2009)  
© 2009 Wiley Periodicals, Inc.

cured formulations). Finally, it was found that fracture properties do not significantly depend either on the hole volume or on the intermolecular interactions. Fracture properties are more dependent on the crosslink density and the glass transition temperature.

© 2009 Wiley Periodicals, Inc. *J Polym Sci Part B: Polym Phys* 47: 1240–1252, 2009

**Keywords:** crosslink density; crosslinking; intermolecular interactions; microstructure-properties relationships; positron annihilation lifetime spectroscopy; thermosets

## INTRODUCTION

Epoxy resins are reactive monomers, which are transformed by curing in thermosetting polymers. Owing to their performance properties, they are extensively used in many applications such as coatings, adhesives, laminates, and matrices for composite materials and structural components. Choosing between the wide variety of curing agents and epoxy resins available, it is possible to tailor and improve polymer properties for specific applications. The functionality of reactants controls the development and the crosslink density of the networks. In this way, it is possible to construct networks of controlled architecture, by only modifying the molecular weight between crosslinks. One way to achieve this modification<sup>1</sup> is by reacting a bifunctional epoxy resin with different functionalities amine mixtures, one of them being a monoamine that plays the role of a chain extender. Thus, the molecular structure of epoxy matrices can be changed in a continuous and controlled mode, from that corresponding to a linear polymer to that for a highly crosslinked polymer.<sup>1–9</sup> Working at epoxy/amine stoichiometric ratio, full reacted networks can be obtained avoiding lateral chains and secondary reactions. Selecting amines with a similar chemical structure, the change in the chemical composition of the system is minimal, and hence the chain flexibility between crosslink points can be retained. Several authors (see for example, refs. 1 and 10) have reported that low deformation mechanical properties measured at a constant temperature, below the glass transition temperature ( $T_g$ ), increase almost linearly with the crosslink density stating that the structure affects them mainly through its influence on  $T_g$ . Other factors such as packing density and chain mobility, including their relationships with the volume variations at nanoscale and their influence on the secondary relaxations are still variables whose effects are not well-known.

Several works have been published studying epoxy/amine mixtures trying to understand the

effects of different variables on their final behavior of this kind of polymers.<sup>1–12</sup> However, most of them have been focused on the effects of the network architecture on their thermal and mechanical behavior and not on the microstructure of the generated networks. The chemical composition, architecture and packing density, chemical interactions, and local mobility of the networks obtained after curing processes are important variables to be analyzed because of their influence on the elastic and fracture properties,<sup>4,5,7,9,11–13</sup> and besides, on the diffusion processes of small molecules through these matrices.<sup>1,14–16</sup> For epoxy networks and other glassy polymers, some works have demonstrated the influence of the test temperature in the glassy state on the nano- and macroscale volumetric behavior using positron annihilation lifetime spectroscopy (PALS) and dilatometry techniques.<sup>17–21</sup>

To advance into the knowledge of the physical facts responsible for variations in the hole volume and specific volume of thermosetting networks, epoxy systems obtained by modification of the crosslink density by partial substitution of the aromatic diamine curing agent with a monoaminic chain extender, with the same chemical composition as the diamine, have been investigated by positron annihilation lifetime spectroscopy and pressure-volume-temperature (PVT)/density measurements.

In a previous work,<sup>22</sup> for a series of aromatic amines with different ring substitution groups and using PALS and PVT measurements, we demonstrated the significant influence of the chemical complexity of the curing agent on the hole volume and also on the specific volume as both clearly increased with the size of the ring substitution groups of the amines.

In this work, trying to understand the role of the intermolecular interactions in these systems, we focused the attention on their effects along with those of crosslink density, packing density, and local mobility on the nanoscopic and macroscopic volumes and also on the mechanical and fracture properties. As we have previously

demonstrated,<sup>23</sup> the use of a selected couple of amines in pre-established concentrations is a reliable method to modify the network architecture from a highly crosslinked network to a linear polymer. In addition, chemical structures of the monoamine–diamine chosen in this work are similar to ensure similar composition of the resultant products, thus avoiding changes in chain flexibility.

## EXPERIMENTAL

### Materials

Epoxy resin used in this study was a bifunctional diglycidyl ether of bisphenol A (DGEBA), DER-332, kindly supplied by Dow Chemical. It has an equivalent weight around 175 g/eq and a hydroxyl/epoxy ratio of 0.015. The diaminic curing agent was 4,4'-diaminodiphenylmethane (DDM), Ciba-Geigy HT972, a solid bifunctional aromatic amine with a molecular weight of 198 g/mol. A solid monofunctional aromatic primary amine, *p*-toluidine, Fluka, with a molecular weight of 107 g/mol, was used as a chain extender. DGEBA was placed in a vacuum oven at 80 °C overnight to remove any water present and amines were used as received without purification. Both of the amines have a similar chemical structure to ensure similar composition of the resultant products.

### Sample Preparation

Epoxy resin was mixed with amine (or amine mixture) at 80 °C stirring vigorously for 5 min keeping stoichiometric epoxy/amine ratio. Amine mixtures were carried out at the following ratios of mono-/diamine equivalents: 100:0, 75:25, 50:50; 25:75, and 0:100 to modify the structure of resultant polymers in a continuous mode. One part of the mixtures was poured into glass tubes previously treated with a demoulding agent, Frekote 44, and preheated to the curing temperature. Cylindrical samples were mechanized to obtain the specimens to be used in PVT measurements. Another part of the mixtures was cast between glass plates coated with Frekote 44 and preheated to the curing temperature in an oven, using vacuum at the first stage, obtaining 2-mm thick samples for PALS measurements and 5-mm thick samples for mechanical properties. Curing of each mixture has been carried out at  $T_{g\infty}-30$  °C until vitrification of each system, being  $T_{g\infty}$  the maximum  $T_g$  achievable for each system measured by differential scanning calorimetry (DSC),<sup>23</sup> and

then at  $T_{g\infty}+30$  °C during 2 h to reach full conversion. Samples corresponding to the system with higher  $T_{g\infty}$  have been postcured at  $T_{g\infty}+20$  °C to avoid their degradation.

## Techniques

### Positron Annihilation Lifetime Spectroscopy Measurements

For PALS measurements, the fast–fast timing coincidence system described elsewhere<sup>16</sup> was used. A time resolution (FWHM) of 255 ps was obtained using the RESOLUTION code.<sup>24</sup> Positron lifetime spectra were recorded at room temperature with a total number of  $2-3 \times 10^6$  coincidence counts using a 0.2 MBq sealed source of <sup>22</sup>NaCl deposited on a thin Kapton foil (7.5 μm). The source was placed between two identical samples with 20 mm square-shaped and 2 mm thickness. According to the common interpretation for PALS measurements in polymers, PALS spectra were deconvoluted into three lifetime components using the LT program,<sup>25</sup> with an adequate source correction. From the analysis, two discrete lifetimes and a continuous one corresponding to the long-lived component were obtained. Positron lifetime spectra were also analyzed using the POSITRONFIT program<sup>24</sup> giving three discrete lifetime components. The results obtained showed a very good agreement with those obtained from the decomposition of the PALS spectra using the LT program. In the last series of decompositions, a discrete lifetime component for the *o*-Ps component ( $\tau_3$ ) was considered.

Lifetime data can be transformed into average sizes of the free volume holes by using the Tao-Eldrup semi-empirical equation.<sup>26,27</sup> The cavity hosting Ps is assumed to be a spherical void with effective radius  $R$ . Such a Ps trap has a potential well with finite depth; however, for convenience of calculations, one usually assumes the depth as infinite, but the radius increased to  $R + \Delta R$ ,  $\Delta R$  (0.166 nm) being an empirical parameter, which describes the penetration of Ps wave function into the bulk.<sup>27</sup> The electron density is supposed to be zero for  $r < R$  and constant for  $r > R$ . The relationship between *o*-Ps lifetime  $\tau_3$  (ns) and radius  $R$  is the following:

$$\tau_3 = 0.5 \left[ \frac{\Delta R}{R + \Delta R} + \frac{1}{2\pi \sin} \left( 2\pi \frac{R}{R + \Delta R} \right) \right]^{-1} \quad (1)$$

The values of the radii obtained from eq 1 should be interpreted only as rough estimates,

because real holes are irregularly shaped. Average volume of holes ( $v_h$ ), as obtained from eq 2, is a key quantity to evaluate the free volume ( $v_f$ ):

$$v_h = \frac{4}{3}\pi R^3 \quad (2)$$

The free volume is defined as:

$$v_f = N_h v_h \quad (3)$$

where  $N_h$  is the number density of holes per mass unit.

### Pressure-Volume-Temperature Measurements

PVT measurements were carried out in a PVT 100 analyzer (SWO/Haake) at room temperature. The samples were placed into the measurement cylinder between PTFE sealings. Specific volume measurements were carried out with a heating rate of 10 °C/min in the range 40–250 °C for the specimens corresponding to systems with higher crosslink densities and 50–250 °C for other systems. 200, 400, 600, and 800 bar pressures were employed in experiments, being 1 bar data extrapolated from them. Results are the average of at least three measurements.

### Differential Scanning Calorimetry

DSC measurements were carried out in a Mettler Toledo calorimeter DSC 821e module equipped with an intracooler, and calibrated with high purity indium and zinc standards. Samples with 5–10 mg were used with nitrogen as purge gas. The glass transition temperature of each system was obtained from the second scan between 30 and 250 °C at 10 °C/min.  $T_g$  values were taken as the middle point of the endothermic shift. Owing to the high vapor pressure of *p*-toluidine, sealed aluminum pans were used.

### Density Measurements

The density ( $\rho$ ) of samples was measured using the Archimedes principle in a Mettler Toledo balance, model AJ50L to obtain the density values, pieces of 2 g obtained from the samples were weighed in air and water, in a temperature controlled environment. Results are the average of at least five measurements.

### Dynamic Mechanical Analysis

Dynamic mechanical analysis (DMA) measurements were carried out in a Perkin–Elmer DMA-7

analyzer using a three point bending device. Secondary relaxations of neat systems have been studied by temperature scans in the range between –150 and 30 °C. Specimens with dimensions 24 × 3 × 1 mm<sup>3</sup> were subjected to a static force of 110 mN and a dynamic force of 100 mN with a span of 15 mm. DMA was also performed from 30 to 250 °C to determine the rubber modulus ( $E_r'$ ) of the systems, as it is an indicative of the molecular weight between crosslinks. Measurements were carried out on specimens of 24 × 3 × 2 mm<sup>3</sup> maintaining a span of 10 mm and using 90 and 80 mN as static and dynamic forces, respectively.  $E_r'$  was measured at a temperature 40 °C higher than that corresponding to the glass transition temperature, taken as the maximum value of the loss tangent in the  $\alpha$  relaxation. All measurements were carried out at a constant frequency of 1 Hz with a heating rate of 5 °C/min using helium atmosphere.

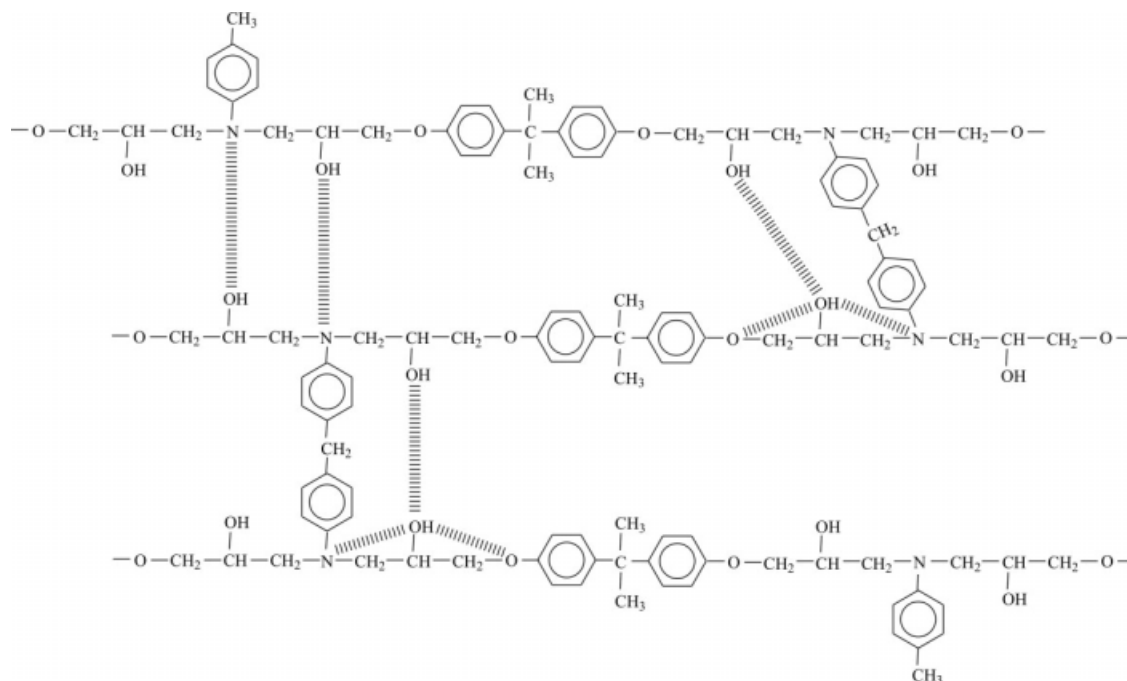
### Fourier Transform Infrared Spectroscopy

Fourier transform infrared spectroscopy (FTIR) analysis was carried out from 4000 to 400 cm<sup>-1</sup> in a Nicolet Nexus 670 spectrometer. The solid was pulverized and mixed with KBr. Twenty scans were taken for each sample with a resolution of 2 cm<sup>-1</sup>.

### Mechanical Properties

Flexural properties were determined in a three point bending device using an Instron universal testing machine, model 4026, equipped with a load cell of 1 kN. Tests were carried out at room temperature with a relative humidity of 50% ± 5% using a crosshead displacement rate of 2.1 mm/min. 100 × 10 × 5 mm<sup>3</sup> specimens were analyzed with a span of 80 mm in accordance with ASTM D-790-93 standard. Results are the average of at least five measurements.

Fracture toughness measurements were analyzed under the same conditions for all samples by determining the critical stress intensity factor ( $K_{IC}$ ) in an Instron universal testing machine, model 4026, equipped with a three point bending device. Obtained results were analyzed in a qualitative mode by using the linear elastic fracture mechanics (LEFM). 60 × 12 × 5 mm<sup>3</sup> specimens were notched with a saw, and a precrack was initiated at the roof of the notch with a razor blade. The notch and crack dimensions were determined by optical microscopy. Tests were carried out at



**Scheme 1.** Schematic representation of several types of hydrogen bonds in epoxy networks.

room temperature with a relative humidity of  $50\% \pm 5\%$  using a crosshead rate of 1.7 mm/min and a span of 48 mm in accordance with ASTM D-5045-91. Results are the average of at least five measurements.

## RESULTS AND DISCUSSION

To avoid the influence of the curing temperature on the network packing density<sup>28</sup> and as described in the Experimental Section, all samples were cured at the same conditions with respect to the  $T_{g\infty}$  values for each system, previously obtained by DSC and reported in ref. 23. Nonetheless, PALS measurements were carried out at room temperature.

The different positions of the testing temperatures with respect to the  $T_g$  values of each system in their glassy states affect both the hole and the specific volumes.<sup>17–21</sup> It is due to the mobility of the epoxy chains of the different systems increases with the proximity to their own  $T_g$ .

Concerning the interpretation of the *o*-Ps lifetime data at temperatures different from  $T_g$ , Jean et al.<sup>21</sup> reported a PALS study on amine-cured epoxy polymers while Consolati et al.<sup>29</sup> studied polyurethanes, these authors focused their works to

the analysis of the evolution of the positron parameters with the temperature. In both papers, it was discussed in detail the *o*-Ps sensitivity to the hole presence depending on the temperature range of measurement with respect to  $T_g$ .

Hydroxyl groups generated during epoxy/amine reactions usually can interact with other functional groups present in the reaction medium. The exact nature of these associations depends on different factors, such as amine nucleophilicity,<sup>30,31</sup> distance between polar species, presence of steric hindrances, temperature, and so forth [14–16,32]. The analysis of interactions is complicated because they can exist between neighboring groups, intramolecular bonds, or with more remote groups, intermolecular bonds.

Intramolecular bonds usually are weaker than the intermolecular ones, because they are not direct links in the sense to preserve the normal angles of the bonds.<sup>33</sup> The main hydrogen bond types that can be formed in epoxy matrices, shown in the Scheme 1, are the association of —OH groups with the tertiary amine located in the crosslink points, or in the case of monoamine connecting linear epoxy units, which can be considered as the stronger interactions taking into account acid–base interactions,<sup>14,15</sup> the association with —O— groups of epoxy resin and the

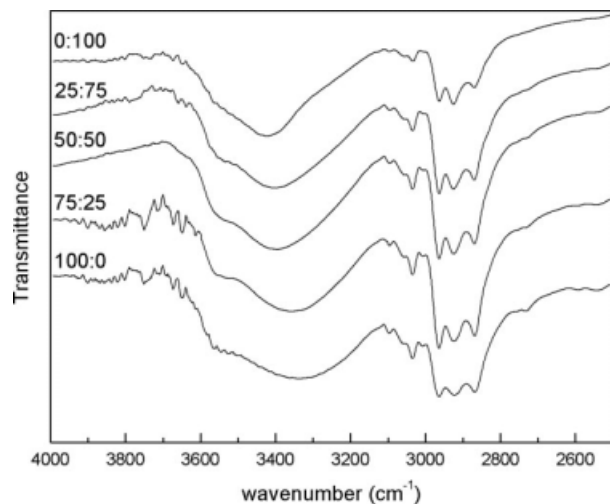


**Figure 1.** FTIR spectra for epoxy systems with several mono-/diamine ratios.

association between two  $\text{—OH}$  groups, but it is difficult to establish the relative extent of each association in a certain system.

Figure 1 shows FTIR spectra between 4000 and 2500  $\text{cm}^{-1}$  of stoichiometric epoxy systems fully cured with different mono-/diamine ratios. The band centered at 3555  $\text{cm}^{-1}$  is attributed to free hydroxyl groups,<sup>31</sup> whereas associated groups show wider and more intense bands displaced to lower wavelength numbers as a consequence of the weakening of the force constants of the covalent bonds in which donor protons take part.

Changing the crosslink density of the systems by increasing the monoamine content, no signifi-

cant variations in the free  $\text{—OH}$  groups position or in the ratio between the intensities of the free  $\text{—OH}$  groups band and associated  $\text{—OH}$  groups band were detected, pointing out that for all systems the amount of these groups remained nearly constant.

Being neighboring groups similar in all analyzed systems, significant variations in the intramolecular interactions are not expected.

On the other hand, the increase in the amount of monoamine caused the displacement of the associated  $\text{—OH}$  broad band to lower wavelength numbers, which can be related to a higher strength of the intermolecular interactions possibly because of a higher bending of chains between crosslink points.

Adding the monoamine, in some way, the presence of the nitrogen atoms in the corresponding extended chains could enhance  $\text{OH—N}$  and also other intermolecular interactions with respect to the nitrogens of the diamines. The *p*-methylphenyl groups linked to the monoaminic nitrogens do not permit the existence of a crosslink point in these nitrogens. As can be seen in the Scheme 1, the nonexistence of a crosslink point causes a lower hindering for the intermolecular interactions at these points by comparison with the nitrogens of the diamines that crosslink the chains.

As shown in Figure 2 for the rubber modulus, the value of this parameter increases together with that representing the crosslink density. A higher amount of monoamine in the curing agent causes the increase of the molecular weight

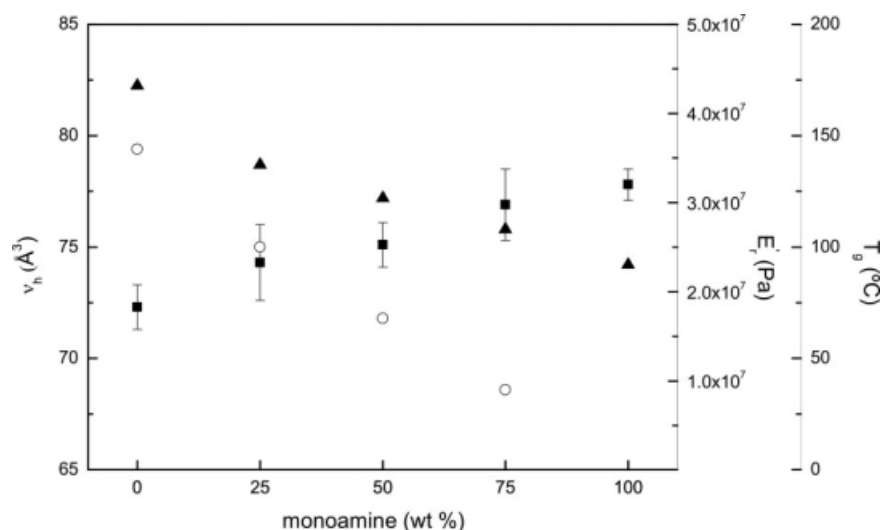


**Figure 2.** (■) Hole volume, (○) rubber moduli, and (▲)  $T_g$  values for epoxy systems as a function of the monoamine content in the curing agent.

between crosslinks, and therefore, the  $T_g$  values (calculated from DSC measurements) decreased as the monoamine acts as a plasticizer for the networks.

In Figure 2, it is also shown the hole volume, obtained from PALS measurements, as a function of the chain extender content for all the systems analyzed. As can be seen, it is worth noting that the  $v_h$  values slightly increased in a steady way when the monoamine content increases. The small differences in the hole volume for the epoxy/diamine system with respect to values previously reported<sup>22,34</sup> can be ascribed to differences in the curing schedule, as pointed out by Salgueiro et al.<sup>28</sup>

For the epoxy network, the increase of the monoamine content in the curing agent formulation only produces small variations of the hole volume. Besides this effect, the monoamine acts as a chain extender, leading to a significant decrease in the crosslink density and also to a decrease in the transition glass temperature. In such a way, four factors seem to be the responsible for the slight variation of the hole volume:

- (i). an increase of the intermolecular interactions through hydrogen bonding should decrease the hole volume and its variations on temperature;
- (ii). a lowering of the crosslink density which slightly increases the hole volume, but this effect has reported to be not significant<sup>34</sup>;
- (iii). the gradient between  $T_g$  and the test temperature used,  $T_g - RT$ , which was lower when the monoamine content increased, should induce to the formation of higher hole volumes for those systems with lower  $T_g$ , that is, with higher monoamine contents. In such a way, PALS results on similar polymers indicated that variations in a certain temperature range near, but below,  $T_g$  could be linked to a mechanism by which Ps is trapped in regions of increasing free volume hole size<sup>21</sup>; and
- (iv). an increase of the added free space induced by the *p*-methylphenyl groups as monoamine content increased. Therefore, the slight increasing tendency of the hole volume on higher monoamine content in the aminic formulation is possibly linked to a compromise among all these effects.

On the basis of the arguments above presented; in Figure 3, the hole volumes for each system

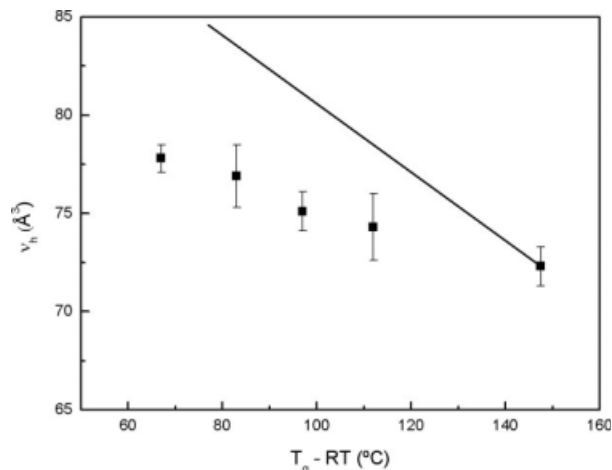


**Figure 3.** (■) Hole volume for epoxy systems as a function of  $T_g - RT$ . The solid line represents the influence of the test temperature with respect to the  $T_g$  of each system using the data published by Monnerie and coworkers<sup>35</sup> for the DGEBA/diamine system.

have been plotted as a function of the gradient  $T_g - RT$ . For comparison, to quantify in an approximate way, the influence of the test temperature with respect to the  $T_g$  of each system, and by assuming the same  $T_g - RT$  variation for the epoxy cured with diamine as that corresponding to each mono-/diamine systems, the hole volume has also been plotted for epoxy/diamine system by means of a straight solid line using the data published by Monnerie and coworkers<sup>35</sup> for this system. A similar line can also be drawn for the specific volume values of this system assuming that its variation follows an expansion law derived from thermodynamics.<sup>19,36</sup> Changes in the gradient between the test temperature and  $T_g$  had a significant influence on the hole volume. In the figure above described, it can be seen that the line representing the hole volume variation on the temperature for epoxy/diamine system goes up for lower gradient  $T_g - RT$  values. By comparing this variation to that shown by the formulations with increasing monoamine content, it can be noted that for each formulation the hole volume was lower than that corresponding to the epoxy/diamine system. Besides, from the other contributions with small effects on the hole volume, as shown above by FTIR, the most significant differences between the formulations appear when the intermolecular interactions increase as monoamine content was higher.

Therefore, we can conclude that the small differences observed in the hole volumes for an

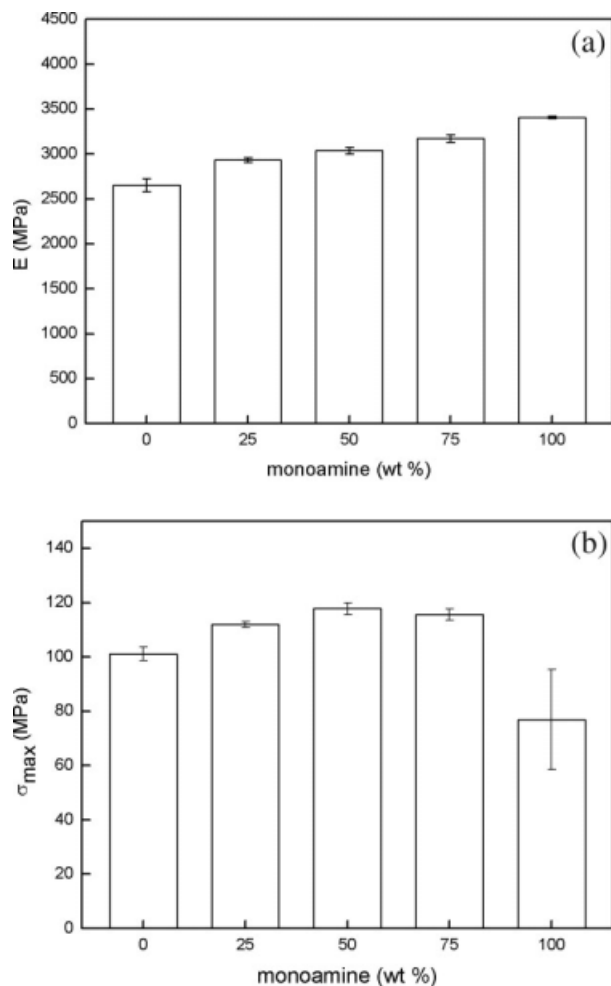


**Figure 4.** (a) Flexural modulus and (b) maximum strength for epoxy systems as a function of the monoamine content in the curing agent.

increasing amount of monoamine in the formulations seem to be mainly related to higher intermolecular hydrogen bonding interactions between chains as a consequence of the more possible adequate accommodation of the monoaminic nitrogens and hydroxyl groups that interact with similar groups of the other chains of the network.

The higher amount of intermolecular interactions via hydrogen bonding for increasing monoamine contents allows to understand not only the mechanical behavior at low deformations observed for the investigated epoxy/mono-diamine systems, shown in Figure 4(a,b), but also our previous results (higher modulus at stoichiometric ratios lower than unity)<sup>37,38</sup> on nonstoichiometric epoxy-diamine formulations and for the modulus diminution at high conversions reported by other authors for stoichiometric epoxy systems as well.<sup>1</sup>

Consequently, both elastic modulus ( $E$ ) and maximum strength ( $\sigma_{\max}$ ) increased as the chain extender content was higher as a consequence of the lower local mobility induced by increasing intermolecular interactions. Thus, the drop in the maximum strength for a 100 wt % monoamine in the aminic formulation may be related to the inhomogeneity and/or the lack of crosslinks of these low molecular weight linear chains.

On the other hand, the significance of the variations mentioned on the local mobility can be better understood when the dynamical mechanical behavior is analyzed in the low temperature range, where the secondary  $\beta$  relaxation corresponding to short-range cooperative motions involving the 2-hydroxypropylether groups occurs.<sup>5,9,11</sup>

From Figure 5(a,b), it becomes evident that the introduction of the chain extender in the aminic formulation diminished this relaxation in both temperature and strength. The onset of the  $\beta$  process occurred at the same temperature for all formulations,<sup>14</sup> but this relaxation broadened toward the high temperature side and increased in strength when the diamine content increases. This behavior induces a higher mobility of 2-hydroxypropylether groups at room temperature when the crosslink density increases. This fact provokes a lower decrease of the storage modulus for the systems with increasing monoamine contents in the temperature range of  $\beta$  relaxation leading to higher values of this property and also of the strength at room temperature. As a result, the introduction of the chain extender plasticizes the system when the  $T_g$  decreases as the monoamine content increases<sup>1</sup> but it also has an antiplasticization effect at low temperatures.

The novelty of our contribution for understanding the variation of the mechanical behavior in epoxy systems is related to the changes of the intermolecular hydrogen bonding interactions between chains, and consequently, on the local mobility, upon the molecular architecture of the networks. This fact can be generalized to explain the mechanical behavior of other epoxy systems, as follows: for crosslinked systems that contain unreacted epoxy groups (epoxy-rich systems—in the case of epoxy-poor mixtures the plasticization effect exerted by the amine excess has also to be taken into account—or not fully cured stoichiometric systems) or for those containing a chain extender as that presented in this work, in which the network monoamine groups not leading to crosslink points allow a higher strength of the



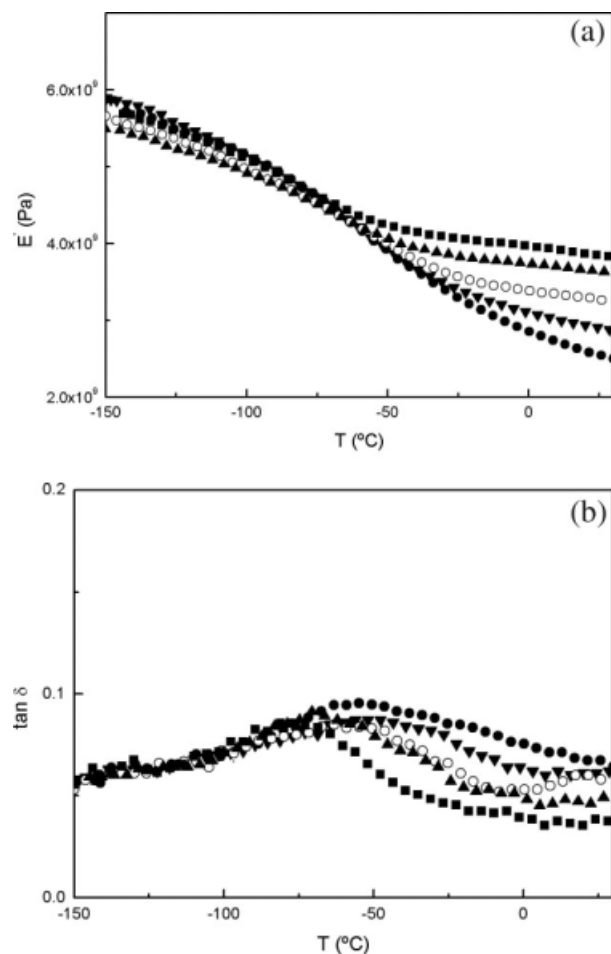


**Figure 5.** (a) Storage modulus and (b) loss tangent obtained by dynamic-mechanical analysis in the range  $-150$  to  $30$   $^{\circ}\text{C}$  for epoxy systems with the mono-/diamine ratios: (●) 0:100, (▼) 25:75, (○) 50:50, (▲) 75:25, and (■) 100:0.

intermolecular hydrogen bonding, their small-range cooperative motions in the region of  $\beta$  relaxation temperatures are hindered (lower broadness and strength of the  $\beta$  relaxation). Therefore, this fact causes an increase (i.e., antiplasticization) of the low-deformation mechanical properties at temperatures between  $\beta$  and  $\alpha$  relaxations.

On the other side, in agreement with results reported by several authors,<sup>1,10</sup> despite the experimental uncertainty of the storage modulus data obtained by DMA, an increasing trend in the modulus can be seen at temperatures below the  $\beta$  relaxation when the crosslink density increases. It can be assigned to the fact that the bulk modulus is more dependent on the cohesive energy.

The fracture behavior of these systems, shown in Figure 6, is more consistent with the plasticization effect, and the decrease in the crosslink den-

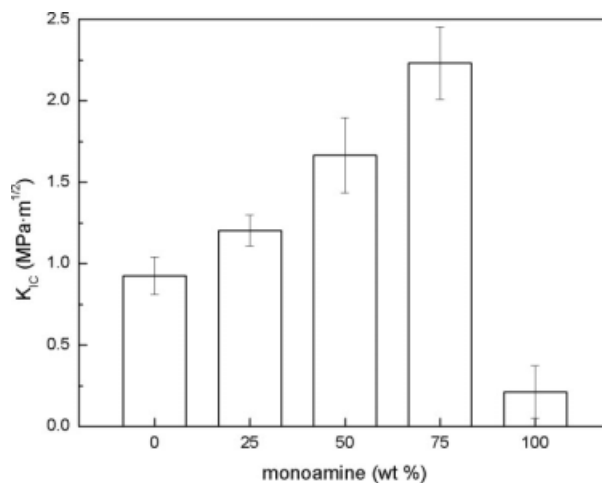


**Figure 6.** Critical stress intensity factor for epoxy systems as a function of the monoamine content in the curing agent.

sity of the networks as the monoamine content in the aminic formulation increase. In consequence, the critical stress intensity factor presents a significant increase for systems with lower  $T_g$  and with lower crosslink density indicating that the hole volume is not a key parameter to determine the fracture properties. Again, the significant drop of the parameters aforementioned for the uncrosslinked epoxy/monoamine system can be related to its inhomogeneities and/or the lack of crosslinks.

On the other hand, the macroscopic changes in the specific volume ( $V_{sp}$ ) were also studied by means of PVT and density measurements. In Figure 7, curves extrapolated to atmospheric

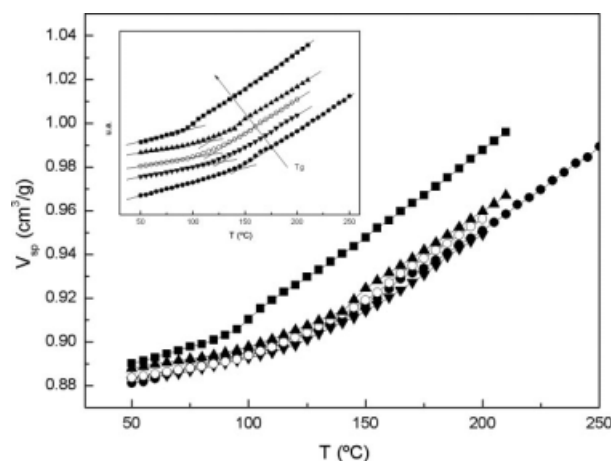


**Figure 7.** Evolution of the specific volume with the temperature at atmospheric pressure for epoxy systems with the mono-/diamine ratios: (●) 100, (▼) 25:75, (○) 50:50, (▲) 75:25, and (■) 100:0.

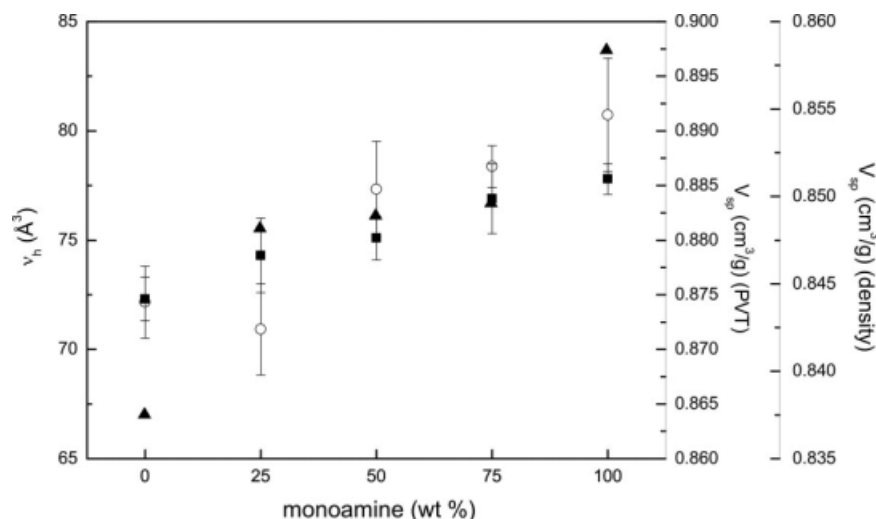


**Figure 8.** Comparison between the hole volume obtained by PALS measurements (■) and the specific volume at room temperature, obtained by PVT measurements at atmospheric pressure (○) and density measurements (▲), for DGEBA/amine systems as a function of the monoamine content in the curing agent.

pressure for one of the samples tested for each monoamine contents are shown. From these curves, specific volume values at room temperature and at atmospheric pressure can be obtained. As can be seen, the change in the slope of the curves, ascribed to  $T_g$ , is displaced to lower temperatures when the monoamine content increases. To highlight the trend and to avoid the overlapping of the curves, other curves have been collected separately in the top inset of Figure 7. For all systems, these curves display a higher variation of the specific volume in the rubbery region than that in the glassy region.

To compare PVT and PALS results, specific volume data measured by both PVT (values extrapolated at 1 bar) and density techniques, and free volume values have been plotted together in Figure 8. As can be seen, increasing the chain extender content in the aminic formulation, the specific volume increased.<sup>4</sup> The increasing tendency observed for both types of volume data ( $v_h$  and  $V_{sp}$ ) points out the close correspondence existing between the macroscopic behavior and the molecular packing of the polymeric chains in thermo-setting networks.

Schmidt and Maurer<sup>39</sup> have reported for poly (methyl methacrylate) an excellent correlation between the specific volume derived from PVT measurements and the size of the free volume cavities  $v_h$  measured by PALS. In a recent work on poly(vinyl chloride) with 10 and 30 wt % of di-

*n*-butyl phthalate as plasticizer, Dlubek et al.<sup>40</sup> showed that the specific volume is related to the number density of holes as:

$$V_{sp} = V_{occ} + V_{fo} + N_h v_h \quad (4)$$

where  $V_{occ}$  is the specific occupied volume,  $N_h$  is the number density of holes per mass unit, being the product  $N_h v_h$  the free volume, and  $V_{fo}$  takes into account a possible deviation of the average volume of the holes estimated from the *o*-Ps lifetime  $\tau_3$ . In this work, we assumed that  $V_{fo} \ll V_{occ}$ .

In previous works,<sup>41–43</sup> it was reported that the  $V_{occ}$  is related to the scaling volume  $V^*$  as follows:

$$V_{occ} = 0.95V^* \quad (5)$$

$V^*$  can be obtained using the Simha-Somcynsky equation of state for polymers<sup>41–44</sup> at atmospheric pressure, which can be approximated by the following universal scaling relationship for  $T > T_g$ :

$$\ln\left(\frac{V_{sp}}{V^*}\right) = B + C\left(\frac{T}{T^*}\right)^{3/2} \quad (6)$$

where  $B = -0.1033$  and  $C = 23.835$  are universal constants;  $V^*$  and  $T^*$  are scaling parameters dependent on the specific structure of the polymer.

In Figure 9, the linear fit of the experimental data at 1 bar, obtained for one of the samples tested, of each monoamine content by using the Simha-Somcynsky equation is reported.  $T^*$  can be

obtained from the slope of the best-fit straight line and  $V^*$  from the ordinate:

$$T^* = \left( \frac{C}{\text{slope}} \right)^{2/3} \quad (7)$$

$$V^* = \exp(\text{ordinate} - B) \quad (8)$$

$V^*$  values so obtained for the different monoamine contents are:  $V^*(0) = 0.833 \pm 0.003$ ;  $V^*(25) = 0.822 \pm 0.013$ ;  $V^*(50) = 0.839 \pm 0.007$ ;  $V^*(75) = 0.839 \pm 0.004$ ;  $V^*(100) = 0.849 \pm 0.005$ .

Using the specific volume data obtained from PVT measurements, the calculated values of the free volume as a function of monoamine content in the curing agent are shown in Figure 10. Taking into account the experimental error, beyond the linear systems, a rather slight increasing tendency of the generated free volume is observed. The free volumes calculated from eqs 4 and 6 have similar values to those shown in Figure 10. These results agree with a previous work where packing density did not change significantly when the crosslink density of the networks changed.<sup>45</sup> However, the small variation of the hole volume for increasing monoamine contents only results in small changes of the free volume of these systems. Thus, only significant variations on the hole volumes, as those shown in a previous work for epoxy systems cured with amines with different chemical structures,<sup>16</sup> result on measurable changes in the free volumes of these systems

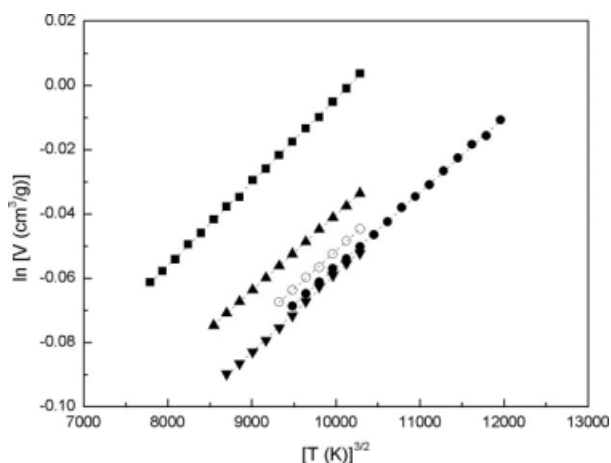


**Figure 9.** Linear fitting of the  $V$ - $T$  experimental data for  $T > T_g$ , using the Simha-Somcynsky equation, for epoxy systems with mono-/diamine ratios: (●) 0:100, (▼) 25:75, (○) 50:50, (▲) 75:25, and (■) 100:0.

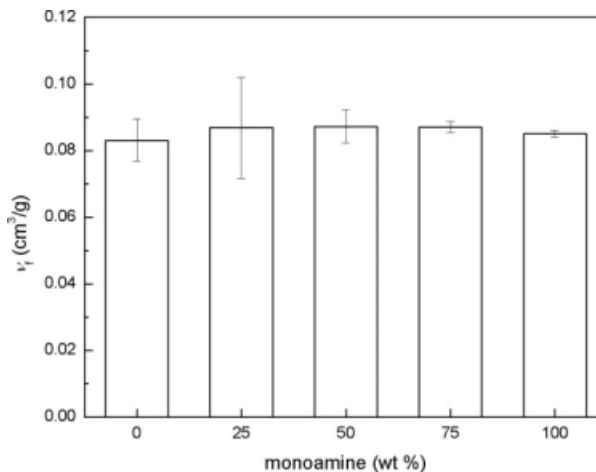


**Figure 10.** Free volume data obtained from PVT measurements for epoxy systems as a function of the monoamine content in the curing agent.

obtained from macroscopic tests as is the case of PVT.

## CONCLUSIONS

The molecular structure of an epoxy matrix has been changed in a controlled mode from that corresponding to a linear polymer to a highly crosslinked polymer, by employing pre-established concentrations of mixtures of a monofunctional aminic chain extender and a bifunctional amine stoichiometrically reacted with a bifunctional epoxy prepolymer. It is worth noting that the chemical structure was identical for all formulations.

Both the average free volume and the specific volume have been analyzed by positron annihilation lifetime spectroscopy and pressure-volume-temperature/density measurements, respectively. It was found that the average hole volume of the networks at room temperature slightly increased when the chain extender content was higher. This increase is produced in a less extent than that expected if the significant change in the molecular structure as the monoamine content increased in the curing agent formulation is taken into account. Accordingly, for epoxy networks with similar chemical composition, the variation of the intermolecular interactions between functional groups of the networks chains, due to the less hindered nitrogen introduced by the monoamine and in some way also to the selected testing conditions; appear to be the responsible for the observed behavior. This conclusion could be

applied to previous investigations of other groups carried out with epoxy matrices not fully cross-linked as a consequence of the use of nonstoichiometric formulations or noncomplete curing conditions.

The increase of the intermolecular interactions at higher monoamine contents leads to a decrease of sub- $T_g$  small-range cooperative motions, which increases the small deformation mechanical properties at temperatures between the  $\beta$  and  $\alpha$  relaxations but not at temperatures below the  $\beta$  relaxation.

Fracture properties do not significantly depend either on the free volumes or on the intermolecular interactions, but they are a function of the crosslink density and the glass transition temperature of the systems.

Macroscopic specific volume also increases with the monoamine content. However, only small variations of the generated free volume have been observed, which points out that for a given epoxy resin the chemical structure of the curing agent is the main responsible for chain packing in the networks developed.

The correlation between PALS and PVT data points out the close relationship between chain molecular packing and the macroscopic behavior in thermosetting networks.

This work was supported by Gobierno Vasco/Eusko Jaurlaritz (S-PE07UN39, IE05-146, and IT-365-07 projects) and Ministerio de Educación y Ciencia/Feder (MAT2006-06331 project). This work was also supported by Universidad de Buenos Aires (UBACYT X-191); Consejo Nacional de Investigaciones Científicas y Técnicas (PIP 5959); Agencia Nacional de Promoción Científica y Tecnológica (PICT 1650/2006 and PID 435/2003); Comisión de Investigaciones Científicas de la Provincia de Buenos Aires; and SECAT-Universidad Nacional del Centro de la Provincia de Buenos Aires, Argentina.

## REFERENCES AND NOTES

- Pascualt, J. P.; Sautereau, H.; Verdu, J.; Williams, R. J. J. *Thermosetting Polymers*; Marcel Dekker: New York, 2002; Chapter 10–12.
- Charlesworth, J. M. *Polym Eng Sci* 1988, 28, 221–229.
- Halary, J. L.; Cukierman, S.; Monnerie, L. *Bull Soc Chim Belg* 1989, 98, 623–634.
- Won, Y. G.; Galy, J.; Gerard, J. F.; Pascualt, J. P.; Bellenger, V.; Verdu, J. *Polymer* 1990, 31, 1787–1792.
- Sindt, O.; Perez, J.; Gerard, J. F. *Polymer* 1996, 37, 2989–2997.
- Fernandez-Nograrro, F.; Llano-Ponte, R.; Mondragon, I. *Polymer* 1996, 37, 1589–1600.
- Mayr, A. E.; Cook, W. D.; Edward, G. H. *Polymer* 1998, 39, 3719–3724.
- Cook, W. D.; Mayr, A. E.; Edward, G. H. *Polymer* 1998, 39, 3725–3733.
- Crawford, E. D.; Lesser, A. J. *J Polym Sci Part B: Polym Phys* 1998, 36, 1371–1382.
- Halary, J. L. *High Perform Polym* 2000, 12, 141–153.
- Lesser, A. J.; Crawford, E. D. *J Appl Polym Sci* 1997, 66, 387–395.
- Crawford, E. D.; Lesser, A. J. *Polym Eng Sci* 1999, 39, 385–392.
- Urbaczewski-Espuche, E.; Galy, J.; Gerard, J. F.; Pascualt, J. P.; Sautereau, H. *Polym Eng Sci* 1991, 31, 1572–1580.
- Soles, C. L.; Yee, A. F. *J Polym Sci Part B: Polym Phys* 2000, 38, 792–802.
- Soles, C. L.; Chang, F. T.; Gidley, D. W.; Yee, A. F. *J Polym Sci Part B: Polym Phys* 2000, 38, 776–791.
- Soles, C. L.; Chang, F. T.; Bolan, B. A.; Hristov, H. A.; Gidley, D. W.; Yee, A. F. *J Polym Sci Part B: Polym Phys* 1998, 36, 3035–3048.
- Jean, Y. C. *Microchem J* 1990, 42, 72–102.
- Wang, C. L.; Hirade, T.; Maurer, F. H. J.; Eldrup, M.; Pedersen, N. J. *J Chem Phys* 1998, 108, 4654–4661.
- Tcharkhtchi, A.; Gouin, E.; Verdu, J. *J Polym Sci Part B: Polym Phys* 2000, 38, 537–543.
- Faupel, F.; Kanzow, J.; Günter-Schade, K.; Nagel, C.; Sperr, P.; Köegel, G. *Mater Sci Forum* 2004, 445, 219–223.
- Jean, Y. C.; Sandreczki, T. C.; Ames, D. P. *J Polym Sci Part B: Polym Phys* 1986, 24, 1247–1258.
- Goyanes, S.; Salgueiro, W.; Somoza, A.; Ramos, J. A.; Mondragon, I. *Polymer* 2004, 45, 6691–6697.
- Blanco, M.; Corcuera, M. A.; Riccardi, C. C.; Mondragon, I. *Polymer* 2005, 46, 7989–8000.
- Kirkegaard, P.; Pedersen, N. J.; Eldrup, M. *PATFIT Program Risoe-M-2740, RNL; Roskilde: Denmark*, 1989.
- Kansy, J. *Mater Sci Forum* 2000, 363, 652–654.
- Tao, S. J. *J Chem Phys* 1972, 56, 5499–5510.
- Eldrup, M.; Lightbody, D.; Sherwood, N. *J Chem Phys* 1981, 63, 51–58.
- Salgueiro, W.; Ramos, J. A.; Somoza, A.; Goyanes, S.; Mondragon, I. *Polymer* 2006, 47, 5066–5070.
- Consolati, G.; Kansy, J.; Pegoraro, M.; Quasso, F.; Zanderighi, L. *Polymer* 1998, 39, 3491–3498.
- Morel, E.; Bellenger, V.; Verdu, J. *Polymer* 1985, 26, 1719–1724.
- Bellenger, V.; Verdu, J.; Francillette, J.; Hoarau, P.; Morel, E. *Polymer* 1987, 28, 1079–1086.

32. He, Y.; Zhu, B.; Inoue, Y. *Prog Polym Sci* 2004, 29, 1021–1051.
33. Nakamoto, K.; Margoshes, M.; Rundle, R. E. *J Am Chem Soc* 1955, 77, 6480–6488.
34. Jeffrey, K.; Pethrick, R. A. *Eur Polym J* 1994, 30, 153–158.
35. Yang, L.; Hristov, H. A.; Yee, A. F.; Gidley, D. W.; Bauchiere, D.; Halary, J. L.; Monnerie, L. *Polymer* 1995, 36, 3997–4003.
36. Bongkee, C. *Polym Eng Sci* 1985, 25, 1135–1138.
37. Mondragon, I.; Quintard, I.; Bucknall, C. B. *Plast Rubber Compos Process Appl* 1995, 23, 331–338.
38. Meyer, F.; Sanz, G.; Eceiza, A.; Mondragon, I.; Mijovic, J. *Polymer* 1995, 36, 1407–1414.
39. Schmidt, M.; Maurer, F. H. J. *Polymer* 2000, 41, 8419–8424.
40. Dlubek, G.; Bodarenko, V.; Pionteck, J.; Supej, M.; Wutzler, A.; Krause-Rehberg, R. *Polymer* 2003, 44, 1921–1926.
41. Utracki, L. A.; Simha, R. *Macromol Theory Simul* 2001, 10, 17–24.
42. Simha, R.; Wilson, P. S. *Macromolecules* 1973, 6, 902–908.
43. Dlubek, G.; Pionteck, J.; Kilburn, D. *Macromol Chem Phys* 2004, 205, 500–511.
44. Simha, R.; Somcynsky, T. *Macromolecules* 1969, 2, 342–351.
45. Won, Y. G.; Galy, J.; Pascault, J. P.; Verdu, J. *Polymer* 1991, 32, 79–83.